J Therm Anal Calorim (2011) 103:1125–1130
DOI 10.1007/s10973-010-1194-x

# Solvation and pairwise association in a 2D fluid

**Giuseppe Graziano**

Received: 26 September 2010 / Accepted: 15 November 2010 / Published online: 24 December 2010


**Abstract** It is shown that it is possible: (a) to derive the 2D scaled particle theory formula of the reversible work of cavity creation using a geometric approach; (b) to obtain the solvation Gibbs energy in a 2D Lennard-Jones fluid; (c) to calculate the solvent contribution to the solvophobic interaction of two Lennard-Jones disks on the basis of geometric arguments. The solvent-excluded surface area associated with cavity creation decreases significantly upon pairwise association, leading to a marked increase in the configurational/translational entropy of solvent disks.

**Keywords** Work of cavity creation · 2D scaled particle theory · Solvophobic interaction · Solvent-excluded surface area

## Introduction

Hydrophobic hydration and hydrophobic interaction are the two main parts of the hydrophobic effect whose molecular/physical origin is still a debated argument [1, 2], and should play a fundamental role for the stability of the folded conformation of globular proteins, the formation of micelles and other aggregates [3–6]. Recently a 2D model of water, the so-called Mercedes-Benz model, originally devised by Ben-Naim [7], has gained credibility due to the Monte Carlo simulation results obtained by Dill and colleagues [8–10]. The Mercedes-Benz model is limited by construction because it is 2D and uses a simplified description of water–water H-bonds. Nevertheless, it is able to produce thermodynamics for the solvation of Lennard-Jones, LJ, disks and for the pairwise association of such disks that are in qualitative agreement with both experimental data and simulation results in detailed water models [8–10]. The success of the Mercedes-Benz water model merits attention and calls for an explanation. In particular, it would be important to try to address the role played by the water–water H-bonds and their reorganization. In fact, Southall and Dill found that the Gibbs energy change for the pairwise association of small LJ disks does not correlate with changes in the number of first shell H-bonds due to enthalpy-entropy compensation [10]. This means that the reorganization of water–water H-bonds as a consequence of pairwise association cannot be the driving force of the process and the latter has to be searched elsewhere. In fact, Southall and Dill showed that the potential of mean force, PMF, of two LJ disks with a radius of 0.35 $l$ (i.e., $l$ is the dimensionless unit length, and 0.35 $l$ is exactly the LJ radius of Mercedes-Benz water disks) can be well reproduced by means of a special application of 2D scaled particle theory [11], SPT, emphasizing that the water–water H-bonds and their reorganization should not play a pivotal role [10].

I would like to go a step further by showing that 2D-SPT can be derived by means of a geometric approach and that this geometric ground explains its ability to qualitatively reproduce the Gibbs energy change upon both solvation and pairwise association of LJ disks in Mercedes-Benz water. Specifically, I would like to show that a suitable geometric application of 2D-SPT is able to produce a PMF for the pairwise association of two large LJ disks (their radius is 1.0 $l$) that is qualitatively similar to that obtained in Mercedes-Benz water by Southall and Dill, and that they did not try to reproduce by means of their special

G. Graziano (✉)
Dipartimento di Scienze Biologiche ed Ambientali,
Università del Sannio, Via Port'Arsa 11, 82100 Benevento, Italy
e-mail: graziano@unisannio.it

application of 2D-SPT [10]. The decrease in solvent-excluded surface area on bringing in contact two disks proves to be the fundamental variable to describe pairwise association in a 2D LJ fluid, because it is a measure of the gain in configurational/translational entropy of solvent disks.

## Theory

According to the statistical mechanical treatment of solvation in real 3D liquids [12, 13], the Ben-Naim standard [14] (i.e., transfer from a fixed position in the gas phase to a fixed position in the liquid phase) Gibbs energy change for the solvation of a LJ disk in a 2D solvent of LJ disks is given by the sum of two contributions:

$$\Delta G^{\bullet} = \Delta G_c + E_a \tag{1}$$

where $\Delta G_c$ is the reversible work to create a cavity suitable to host the solute [15], and $E_a$ is the energy gain for turning on solute–solvent interactions; a term due to the solvent reorganization upon solute insertion is not present because enthalpy–entropy compensation is operative [12, 13]. Note that in the rest of the article all the Gibbs energy terms are normalized to the random thermal energy $kT$, so to have dimensionless quantities.

It is possible to provide a geometric derivation of the SPT formula to calculate the reversible work of cavity creation in a 2D hard disk fluid, following the same approach used in the case of 3D hard sphere fluids [16, 17]. In general, it has to be noted that there are two measures of cavity size: (a) the radius of the circular region from which all parts of the fluid disks are excluded, indicated by $r_c$; (b) the radius of the circular region from which the centres of the fluid disks are excluded, indicated by $R_c$; for circular cavities $R_c = r_c + r_1$, where $r_1$ is the radius of the fluid hard disks. In analogy with the definition of the solvent accessible surface area [18], SASA, in 3D, it is possible to define the solvent accessible perimeter, SAP, in 2D; for circular cavities SAP $= 2\pi R_c$.

According to a general theorem of statistical mechanics [19], the reversible work of cavity creation is exactly related to the probability of finding no centres of solvent molecules in the desired circular region of $R_c$ radius, $p_0(R_c)$, also called insertion probability (note that the location of the cavity has to be fixed, but arbitrarily in the system because the fluid density is uniform at equilibrium):

$$\Delta G_c/kT = -\ln p_0(R_c) \tag{2}$$

Simple geometric arguments indicate that, for $0 \le R_c \le r_1$, at most one disk centre can be found in the cavity, so that $p_0(R_c)$ can readily be obtained, leading to the following exact relationship:

$$\Delta G_c/kT = -\ln(1 - \pi \cdot \rho_1 \cdot R_c^2) \tag{3}$$

where $\rho_1$ is the number density of the 2D fluid, number of disks for the square of the unit length indicated by $l$, and considered to be dimensionless. For cavities having $R_c \ge r_1$, the insertion probability $p_0(R_c)$ can be expressed as the ratio between the ensemble average surface area available to insert such a cavity and the total surface area of the 2D fluid, so that:

$$\Delta G_c/kT = -\ln[\langle A_{avail}(R_c)\rangle/A_{tot}] \tag{4}$$

where $A_{tot} = 1/\rho_1$, while $\langle A_{avail}(R_c)\rangle$ is a statistical mechanical term that measures only the void area whose dimensions allow the occurrence-insertion of a cavity of $R_c$ radius; $\langle A_{avail}(R_c)\rangle$ is not a constant quantity for a given 2D fluid, but it depends on the selected $R_c$ value. To a first approximation, valid at low fluid densities, $\langle A_{avail}(R_c)\rangle$ can be related to the area excluded to each fluid disk of $r_1$ radius for the presence of the cavity by the following relationship:

$$\langle A_{avail}(R_c)\rangle = A_{tot} - [N_1 \cdot a_{ex}(r_1, r_c)] \tag{5}$$

where $N_1$ is the number of disks of $r_1$ radius in the $A_{tot}$ surface area; $a_{ex}(r_1, r_c)$ is the area excluded to each disk of $r_1$ radius due to the insertion of a circular cavity of $r_c$ radius. Since $a_{ex}(r_1, r_c) = \pi(r_1 + r_c)^2$, and by defining the surface packing fraction $\eta = (\pi \cdot r_1^2/A_{tot})$, the insertion probability, after some rearrangements, becomes:

$$p_0(r_c) = (1-\eta) \cdot \{1 - [2\eta/(1-\eta)] \cdot (r_c/r_1) - [\eta/(1-\eta)] \cdot (r_c/r_1)^2\} \tag{6}$$

By putting the latter into Eq. 2, and expanding the logarithm in powers of $r_c$ up to the linear term, one obtains:

$$\Delta G_c/kT = -\ln(1-\eta) + [2\eta/(1-\eta)] \cdot (r_c/r_1) \tag{7}$$

In the condition of constant pressure and temperature, upon insertion of a cavity of $r_c$ radius, the total surface area of the hard disk fluid increases by a quantity corresponding to the molar area of the inserted cavity [16, 17] (more correctly, in a real 2D fluid, the partial molar area of the inserted cavity). The latter area multiplied by the pressure of the hard disk fluid gives a further contribution that should be added to Eq. 7 to obtain a full expression for $\Delta G_c/kT$. According to SPT [20, 21], the pressure of a 2D hard disk fluid is:

$$P/kT \cdot \rho_1 = 1/(1-\eta)^2 \tag{8}$$

and the $\Delta G_c/kT$ expression proves to be:

$$\Delta G_c/kT = -\ln(1-\eta) + [2\eta(/(1-\eta)] \cdot (r_c/r_1) + \left[\eta/(1-\eta)^2\right] \cdot (r_c/r_1)^2 \tag{9}$$

This formula exactly corresponds to that derived by means of a classic SPT approach by Helfand et al. [22].

Note that the quadratic term obtained from the power series expansion of Eqs. 2 and 6 is not correct [i.e., the pressure would be $P/kT{\cdot}\rho_1 = (1+\eta)/(1-\eta)^2$]; it is too large probably because the $\langle A_{\text{avail}}(R_c)\rangle$ expression of Eq. 5 does not take into account, in a correct manner, the non-overlap condition for the solvent disks contacting the cavity perimeter.

Another key quantity, the cavity contact correlation function, $G(R_c)$, which is the conditional solvent density just outside a circular cavity of $R_c$ radius, is given by [19]:

$$G(R_c) = (1/2\pi \cdot \rho_1 \cdot R_c) \cdot [\partial(\Delta G_c/kT)/\partial R_c] \tag{10}$$

By applying Eq. 10 to the expressions in Eqs. 3 and 9, the cavity contact correlation function proves to be:

$$G(0 \le R_c \le r_1) = 1/[1 - \pi \cdot \rho_1 \cdot R_c^2] \tag{11}$$

$$G(R_c \ge r_1) = (1/\pi \cdot \rho_1 \cdot R_c) \cdot [\eta/(1-\eta) \cdot r_1] + [\eta \cdot r_c/(1-\eta)^2 \cdot r_1^2] \tag{12}$$

The $E_a/kT$ term has to account for the energetic interactions of a LJ disk solute in a fluid of LJ disks. It can be calculated by using a simple formula derived following the procedure devised by Pierotti in 3D [23]. In the assumption that the solvent density at contact with the solute is two times that of bulk solvent (for more on this point see the "Results and Discussion" section), the formula is:

$$E_a/kT = -(48/5) \cdot \eta \cdot (\varepsilon_1 \cdot \varepsilon_2)^{1/2} \cdot [(r_1 + r_2)/2 \cdot r_1]^2 \tag{13}$$

where $\varepsilon_1$ and $\varepsilon_2$ are the Lennard-Jones potential parameters for the solvent and solute, respectively, measuring the magnitude of the maximum attractive potential energy and assumed to be dimensionless. This formula is physically sound, and should perform satisfactorily also in 2D.

Following geometric arguments developed in 3D systems [24, 25], for the pairwise association of two LJ disks in a 2D fluid of LJ disks, the solvent contribution to the Gibbs energy of the solvophobic interaction, $\delta G(\text{SI})/kT$, can be calculated from the knowledge of SAP buried upon association:

$$\delta G(\text{SI})/kT = [(\Delta G_c/kT \cdot \text{SAP}) + (E_a/kT \cdot \text{SAP})] \cdot \Delta\text{SAP}\,(\text{association}) \tag{14}$$

The SAP buried upon association is a negative quantity; the $\Delta G_c/kT{\cdot}$SAP ratio is a positive quantity favouring pairwise association; the $E_a/kT{\cdot}$SAP ratio is a negative quantity contrasting pairwise association. The rationale is that bringing two LJ disks from a fixed position at infinite distance to a fixed position at contact distance in a 2D solvent causes: (a) a decrease in the solvent-excluded area, measured by the SAP decrease upon association, that produces a significant gain of configurational/translational entropy of solvent disks; (b) a decrease in the number of solvent disks contacting the two LJ disk solutes, that leads to a significant loss of favourable solute–solvent energetic interactions [26].

The fraction of total SAP buried on bringing two disks from infinite separation into close contact can be calculated in an analytic way by means of the following formula derived from a simple geometric construction:

$$f_{\text{SAP}} = \arccos[r_{AB}/2 \cdot (r_1 + r_2)]/\pi \tag{15}$$

where $r_{AB}$ is the distance between the centres of the A and B solute disks; $r_{AB}$ cannot be smaller than $2{\cdot}r_2$ (corresponding to the contact configuration of the two disks). It is worth noting that $f_{\text{SAP}}$ depends on the size of the two approaching disks (because the radius of the solvent disk is fixed; $r_1 = 0.35\ l$ in this work), decreasing significantly on increasing their radius. For the case considered in the present study, $r_2 = 1.0\ l$, $f_{\text{SAP}} = 0.087$ at $r_{AB} = 2.6\ l$, 0.176 at $r_{AB} = 2.3\ l$, and 0.234 at $r_{AB} = 2.0\ l$. Thus, it is straightforward to calculate:

$$\Delta\text{SAP}(\text{association}) = -4\pi(r_1 + r_2) \cdot f_{\text{SAP}} \tag{16}$$

and so to obtain estimates of $\delta G(\text{SI})/kT$ as a function of $r_{AB}$.

## Results and discussion

2D-SPT calculations have been performed in a hard disk fluid having a number density $\rho_1 = 0.9$ disks/$l^2$ and a disk radius $r_1 = 0.35\ l$, so that the surface packing density $\eta = 0.3464$; these numbers correspond to those originally selected by Ben-Naim for the so-called Mercedes-Benz water [7]. The trend of the $\Delta G_c/kT$ function is shown in Fig. 1: curve *a* has been obtained by means of Eq. 3 and the full expression of Eq. 9; curve *b* has been obtained by neglecting the quadratic term corresponding to the pressure-area work in Eq. 9. The $\Delta G_c/kT$ function is always

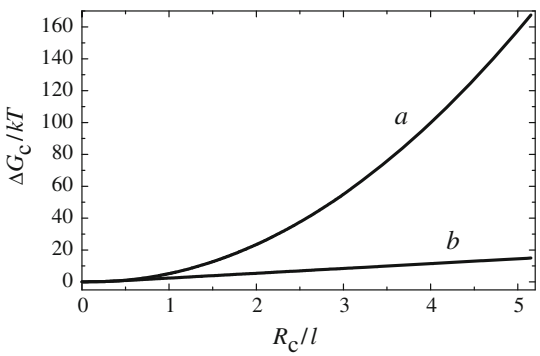


**Fig. 1** Trend of $\Delta G_c/kT$ versus $R_c$ by taking into account the pressure-area work contribution (curve *a*), or neglecting it (curve *b*). See text for further details

increasing as expected, and Fig. 1 emphasizes that the quadratic term provides a very large contribution to $\Delta G_c/kT$. This is readily confirmed by looking at the $G(R_c)$ function, whose trend is shown in Fig. 2: curve *a* has been calculated by means of Eqs. 11 and 12, whereas curve *b* has been calculated by neglecting the last term in Eq. 12, that originates from the pressure-area work contribution. The $G(R_c)$ function is continuously increasing in the case of curve *a*, even though it seems to level off at a value of about 2.6 for large $R_c$ values, whereas it reaches a maximum at $R_c = 0.35\ l$, and then decreases continuously in the case of curve *b*. In other words, on increasing the cavity radius, in the first case, circular cavities prove to be wetted by solvent disks, whereas, in the second case, they prove to be de-wetted by solvent disks. This marked difference confirms the major role played by the pressure-area work contribution. The finding that, by taking into account the pressure-area work contribution, the density of solvent disks contacting the cavity perimeter is almost always two times that of bulk solvent has been the ground for the assumption made in deriving the $E_a/kT$ expression in Eq. 13.

The trend of the $\Delta G_c/kT{\cdot}SAP$ function is shown in Fig. 3: the function proves to be always linearly increasing by considering Eq. 3 and the full expression of Eq. 9, as shown by curve *a*; whereas it reaches a plateau for large $R_c$ values by neglecting the pressure-area work contribution in Eq. 9, as shown by curve *b*. In the case of 2D Mercedes-Benz water, the $\Delta G_c/kT{\cdot}SAP$ function, calculated by means of Monte Carlo simulations, showed a plateau for large $R_c$ values [9], probably because the pressure is very low in such a fluid due to the existence of strong H-bonds.

For the Ben-Naim standard solvation Gibbs energy of a LJ disk with $r_2 = 1.0\ l$ and $\varepsilon_2 = 0.1$ in a LJ disk fluid having $\rho_1 = 0.9$ disks/$l^2$, $r_1 = 0.35\ l$ and $\varepsilon_1 = 0.1$, by applying Eqs. 9 and 13, one obtains: $\Delta G^{\bullet}/kT = (\Delta G_c/kT) + (E_a/kT) = 10.07 - 1.24 = 8.83$. This large positive $\Delta G^{\bullet}/kT$ value emphasizes the solvophobic nature of the process; its magnitude, however, proves to be significantly larger than that calculated in Mercedes-Benz water due to the pressure-area work contribution. The $\Delta G_c/kT$ term proves to be dominant due to the small size of fluid disks and the high number density of the fluid (i.e., the two special features of water [12, 13, 17], and of Mercedes-Benz water). On increasing the strength of the solute–solvent energetic interactions, by keeping fixed all the other parameters, the $\Delta G^{\bullet}/kT$ value would decrease and eventually could become also negative.

The solvent contribution to the solvophobic interaction of two LJ disks having $r_2 = 1.0\ l$ and $\varepsilon_2 = 0.1$ in a LJ disk fluid having $\rho_1 = 0.9$ disks/$l^2$, $r_1 = 0.35\ l$ and $\varepsilon_1 = 0.1$, has been calculated by means of Eqs. 14–16 as a function of the disk centre–disk centre separation. The obtained trends are shown in Fig. 4. It is evident that the $[\Delta G_c/kT{\cdot}\mathrm{SAP}]{\cdot}\Delta\mathrm{SAP}(\mathrm{association})$ term (curve *a*) provides a

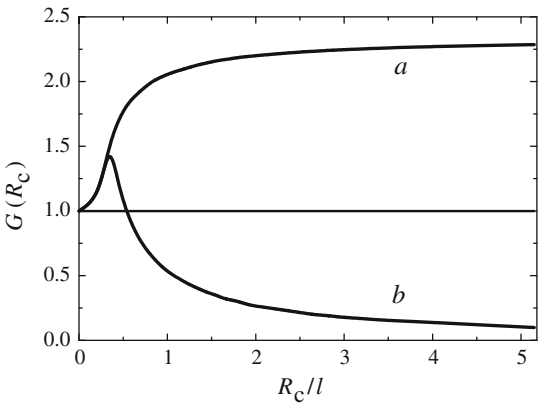


**Fig. 2** Trend of the cavity contact correlation function $G(R_c)$ versus $R_c$ by taking into account the pressure-area work contribution (curve *a*), or neglecting it (curve *b*). See text for further details

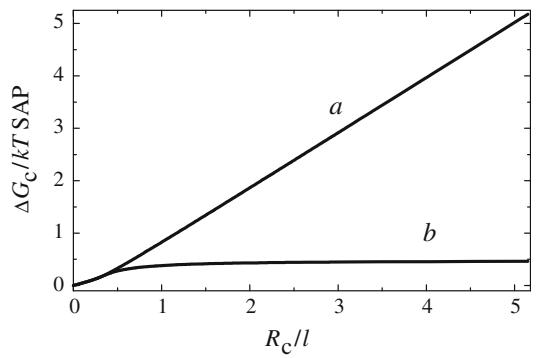


**Fig. 3** Trend of $\Delta G_c/kT{\cdot}SAP$ versus $R_c$ by taking into account the pressure-area work contribution (curve *a*), or neglecting it (curve *b*). See text for further details

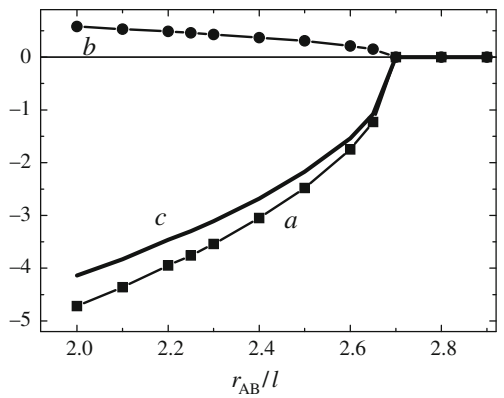


**Fig. 4** Dependence of the $[\Delta G_c/kT{\cdot}SAP]{\cdot}\Delta SAP(\mathrm{association})$ term (curve *a*), the $[E_a/kT{\cdot}SAP]{\cdot}\Delta SAP(\mathrm{association})$ term (curve *b*), and the solvent contribution $\delta G(\mathrm{SI})/kT$ to pairwise association (curve *c*) on the disk centre–disk centre distance $r_{AB}$. See text for further details

large negative contribution that overwhelms the small positive contribution of the $[E_a/kT{\cdot}\mathrm{SAP}]{\cdot}\Delta SAP$(association) term (curve *b*). This means that the SAP decrease upon disk association (that is an effective measure of the decrease in the solvent-excluded surface area) causes a so large gain in configurational/translational entropy for solvent disks to drive pairwise association [24]. This result is a consequence of the small size of solvent disks and the large number density of the solvent: both these features are characteristic of real water. The trend of $\delta G(\mathrm{SI})/kT$ versus $r_{AB}$ (i.e., the calculated PMF, curve *c*) is qualitatively similar to that obtained for the same LJ disks in the Mercedes-Benz water by Southall and Dill, performing NPT Monte Carlo simulations (see Fig. 10 in Ref. [10]). The approximately linear decrease of the Gibbs energy on bringing in contact the two disks has to be considered a clear indication that ΔSAP is the right variable to describe the process also in Mercedes-Benz water [i.e., the geometric arguments leading to Eqs. 14–16 are right]. It is worth noting that I have already shown that a similar geometric approach is able to shed light on the conformational stability of globular proteins, in particular on the occurrence of cold denaturation [27].

The quantitative discrepancy for the stability of the contact configuration at $r_{AB} = 2.1\ l$, $\delta G(\mathrm{SI})/kT = -1.8$ in the Mercedes-Benz water versus −3.8 with the present procedure, is surely because the pressure-area work contribution is too large in the 2D hard sphere fluid. The fact that the PMF calculated by Southall and Dill starts to be negative at $r_{AB} \approx 3.0\ l$ (see Fig. 10 in Ref. [10]), whereas the present one starts to be negative at $r_{AB} \approx 2.7\ l$ (see curve *c* in Fig. 4), is a simple consequence of a specific feature of Mercedes-Benz water disks. They have two size measures by construction [7–10]: the LJ radius of 0.35 *l*, and the H-bond radius of 0.5 *l*; this feature affects $f_{SAP}$ because the latter depends on the solvent disk radius, as indicated by Eq. 15.

A final point merits attention. The hydration shell of the LJ disk with $r_2 = 1.0\ l$ consists of about 10 Mercedes-Benz water disks and so about 10 water–water H-bonds (see Fig. 11 in Ref. [10]). The hydration shell of two such LJ disks in the contact configuration consists of about 14 Mercedes-Benz water disks for a net loss of about 6 water–water H-bonds with respect to the separated configuration of the two LJ disks. In view of the energetic strength of H-bonds in Mercedes-Benz water [8–10], such a loss should render unfavourable pairwise association. But this is not the case, as shown by the Monte Carlo simulation results [10], because the reorganization of water–water H-bonds is characterized by an almost complete enthalpy–entropy compensation [12, 13, 17, 28], and the overall Gibbs energy is dominated by the gain in configurational/translational entropy of Mercedes-Benz water disks for the decrease in solvent-excluded surface area (i.e., the SAP decrease) on bringing in contact the two LJ disks.

In conclusion, I have shown that it is possible: (a) to derive the 2D-SPT formula of $\Delta G_c$ by using a geometric approach; (b) to obtain the solvation Gibbs energy in a 2D LJ fluid; (c) to calculate the solvent contribution to the solvophobic interaction of two LJ disks on the basis of geometric arguments. The solvent-excluded surface area associated with cavity creation decreases significantly upon pairwise association, leading to a marked increase in the configurational/translational entropy of solvent disks.

## References


1. Blokzijl W, Engberts JBFN. Hydrophobic effects. Opinions and facts. Angew Chem Int Ed Engl. 1993;32:1545–79.
2. Chandler D. Interfaces and the driving force of hydrophobic assembly. Nature. 2005;437:640–7.
3. Graziano G. Is there a relationship between protein thermal stability and the denaturation heat capacity change? J Therm Anal Calorim. 2008;93:429–38.
4. Taheri-Kafrani A, Bordbar AK. Energetics of micellization of sodium *n*-dodecyl sulfate at physiological conditions using isothermal titration calorimetry. J Therm Anal Calorim. 2009;98:567–75.
5. Galan JJ, Rodriguez JR. Thermodynamic study of the process of micellization of long chain alkyl pyridinium salts in aqueous solution. J Therm Anal Calorim. 2010;101:359–64.
6. Desii A, Duce C, Ghezzi L, Monti S, Solaro R, Tinè MR. Investigation of the self-assembly of hydrophobic self-complementary ionic tetrapeptides. J Therm Anal Calorim. 2009;97:791–6.
7. Ben-Naim A. Statistical mechanics of "waterlike" particles in two dimensions: I Physical model and application of the Percus-Yevick equation. J Chem Phys. 1971;54:3682–95.
8. Silverstein KAT, Haymet ADJ, Dill KA. A simple model of water and the hydrophobic effect. J Am Chem Soc. 1998;120:3166–75.
9. Southall NT, Dill KA. The mechanism of hydrophobic solvation depends on solute radius. J Phys Chem B. 2000;104:1326–31.
10. Southall NT, Dill KA. Potential of mean force between two hydrophobic solutes in water. Biophys Chem. 2002;101–102:295–307.
11. Reiss H, Frisch HL, Lebowitz JL. Statistical mechanics of rigid spheres. J Chem Phys. 1959;31:369–80.
12. Lee B. Solvent reorganization contribution to the transfer thermodynamics of small nonpolar molecules. Biopolymers. 1991;31:993–1008.
13. Graziano G. Benzene solubility in water: a reassessment. Chem Phys Lett. 2006;429:114–8.
14. Ben-Naim A. Solvation thermodynamics. New York: Plenum Press; 1987.
15. Graziano G. Water's surface tension and cavity thermodynamics. J Therm Anal Calorim. 2008;91:73–7.
16. Graziano G. A purely geometric derivation of the scaled particle theory formula for the work of cavity creation in a liquid. Chem Phys Lett. 2007;440:221–3.
17. Graziano G. Salting out of methane by sodium chloride: a scaled particle theory study. J Chem Phys. 2008;129:084506.

18. Lee B, Richards FM. The interpretation of protein structures: estimation of static accessibility. J Mol Biol. 1971;55:379–400.
19. Reiss H. Scaled particle methods in the statistical thermodynamics of fluids. Adv Chem Phys. 1966;9:1–84.
20. Boublik T. Two-dimensional convex particle liquid. Mol Phys. 1975;29:421–8.
21. Talbot J, Tildesley DJ. The planar dumbbell fluid. J Chem Phys. 1985;83:6419–24.
22. Helfand E, Frisch HL, Lebowitz JL. Theory of the two- and one-dimensional rigid sphere fluids. J Chem Phys. 1961;34:1037–42.
23. Pierotti RA. A scaled particle theory of aqueous and nonaqueous solutions. Chem Rev. 1976;76:717–26.
24. Graziano G. Dimerization thermodynamics of large hydrophobic plates: a scaled particle theory study. J Phys Chem B. 2009;113:11232–9.
25. Graziano G. Role of salts on the strength of pairwise hydrophobic interaction. Chem Phys Lett. 2009;483:67–71.
26. Graziano G. Hydrophobic interaction of two large plates: an analysis of salting-in/salting-out effects. Chem Phys Lett. 2010;491:54–8.
27. Graziano G. On the molecular origin of cold denaturation of globular proteins. Phys Chem Chem Phys. 2010;12:14245–52.
28. Lee B, Graziano G. A two-state model of hydrophobic hydration that produces compensating enthalpy and entropy changes. J Am Chem Soc. 1996;118:5163–8.